Operational analysis of the spatial distribution and the temporal evolution of the snowpack water equivalent in southern Québec, Canada

R. Turcotte[1,4], L.-G. Fortin[2], V. Fortin[3], J.-P. Fortin[4] and J.-P. Villeneuve[4]

[1]Division de l'Expertise Hydrométéorologique, Direction de l'Expertise Hydrique et de la Gestion des Barrages Publics, Centre d'Expertise Hydrique du Québec, Ministère du Développement Durable et de l'Environnement et des Parcs, 675 Boul. René-Lévesque Est, Aile René-Lévesque Est, RC, Boîte 28, Québec G1R 5V7, Canada. E-mail: *richard.turcotte@mddep.gourv.qc.ca*

[2]Centre d'Expertise Hydrique du Québec, G1R 5V7, Canada

[3]Numerical Weather Prediction Research, Meteorological Research Division, Environment Canada, Dorval H9P 1J3, Canada

[4]Institut National de la Recherche Scientifique, Centre Eau, Terre et Environnement, Québec G1K 9A9, Canada

Received 26 January 2006; accepted in revised form 12 December 2006

Abstract A technique for obtaining an operational regional analysis of the temporal evolution of the snowpack water equivalent in southern Québec (Canada) is proposed and implemented on a 0.1° grid. The technique combines the output of the snowpack model included in the HYDROTEL hydrological model, forced by observed temperatures and precipitations, with observed snow survey data. A strategy based on observed snow density, snowpack water equivalent and streamflow is used for model calibration. A comparison of various calibration strategies showed that the same model parameters can be used for the whole of southern Québec. It was also shown that, for operational purposes, it is sufficient to rely solely on automatic stations and to use 3 h time steps. Because snow surveys are made in deciduous forests, model parameters were adjusted to account for open areas and coniferous trees by comparing observed and simulated streamflow, using all components of the hydrological model. An assimilation technique which updates simulated water equivalent and snow density at grid points from the available snow survey data completes the operational system. An example of spring streamflow simulated using the proposed snow analysis illustrates the usefulness of the technique.

Keywords Assimilation of snow data; operational snow analysis; snow hydrology; snow model calibration

Introduction

Accurate hydrological forecasting of streamflow and reservoir inflows is critical for properly managing major hydrologic events such as floods and droughts (WMO (World Meteorological Organization) 1992). In particular, hydrological forecasts serve to alert the stakeholders and the authorities and enable prompt disaster warning. In the spring, an accurate assessment of the snowpack water equivalent (SWE) on the basin is very important for accurate flow forecasting during snow melt. Operational availability of SWE analysis on a daily basis is a major part of flood mitigations.

In contrast with western Canadian provinces and territories and the US, there is no snow pillow measurement program in Québec. The manual snow survey network is still the most reliable observation source for SWE. Techniques proposed for deriving a SWE analysis through interpolation of snow survey observations (e.g. Tapsoba *et al.* 2005; Seidou *et al.* 2006) are therefore not applicable, because of the low temporal resolution of the snow survey network (roughly one observation every two weeks), with a schedule varying from station to

Nordic Hydrology **Vol 38 No 3 pp 211–234** © IWA Publishing 2007

doi: 10.2166/nh.2007.009

station), and also because of the low spatial resolution of this network in Southern Québec. It is thus necessary to complement the direct observations of SWE obtained from the snow survey network with other indirect sources of information on SWE that could be available on a daily basis.

While operational mapping of snow cover extent is now common (e.g. Romanov 2003; Woo and Young 2004; Simic *et al.* 2004), operational products for daily SWE assessment are still rare. Research and operational products for SWE assessment can be divided into four categories: remote sensing products; operational SWE analyses used by existing Numerical Weather Prediction Systems; outputs from land data assimilation systems (LDAS) forced by analyses of surface variables; and results from snow models forced by observations of precipitation and air temperature.

Some success with remote sensing has been obtained for SWE estimation over the flat and low vegetated Canadian prairies (Goïta *et al.* 2003). However, several studies show that it remains a difficult problem to solve in more complex terrain (Derksen *et al.* 2003). Research projects involving remote sensing in Québec, relying either on active microwave measurements (Bernier *et al.* 1999) or on passive microwave observations (De Sève *et al.* 2001; Roy 2004), are primarily intended to assess SWE in the northern part of the province and cannot easily be transposed to southern Québec conditions (Brown *et al.* 2000) for the same reasons. Airborne gamma remote sensing, such as in use at the NWS (Carroll *et al.* 2000), is expensive and difficult to use in hilly and forested areas, which are common in southern Québec. It is therefore unlikely that operational remote sensing products will be available anytime soon for SWE assessment in southern Québec.

Snow analyses are available for use in numerical weather prediction (NWP) systems (Brasnett 1999). They are generally obtained by combining a first guess generated by the NWP system with snow depth observations. However, because focus is put on snow depth in the analysis process, not SWE, the error on SWE can be high. Furthermore, the resolution of the atmospheric model used to obtain the first guess is still fairly low. For example, an ongoing study by Fortin *et al.* (2006*a*) showed that current errors in the operational SWE analysis available from the Canadian Meteorological Centre (CMC) and used as a lower bound condition by the GEM meteorological model (Bélair *et al.* 2003) are far too large for hydrological uses in Southern Québec, with a root mean square error of about 100 mm for SWE.

Land data assimilation systems (LDAS) offer the possibility of combining high-resolution analyses of surface variables with a high-resolution land-surface scheme (LSS), which would typically include an energy-balance snow model, to generate simulations of surface variables, including snow water equivalent (Pietroniro *et al.* 2006). While an experimental analysis of liquid precipitation is available for Canada (Mahfouf *et al.* 2007), an analysis of solid precipitation still has to be developed. Hence, while this approach is promising, validated results from a LDAS in Canada are still a few years away. In addition, challenges associated with the assimilation of snow survey observations in LDAS have not been addressed yet.

The possibility remains to force a simpler snow model with observed precipitation and temperature to provide an estimate of SWE. This modelling technique has been used with success by Brown *et al.* (2003). We shall now discuss how to take this approach a step further by combining this first guess with observations of SWE.

Given the results of the literature review, we propose in this paper an operational approach that combines *in situ* observations of SWE and snow depth from a snow survey network, with a mathematical model which simulates the temporal evolution of the snowpack, using precipitation and air temperature as inputs. The snow survey observations are used to update some state variables of the mathematical model (SWE and snow depth). By combining the model and the observations, the SWE can be estimated at each point of the

spatio-temporal domain, despite the fact that these observations have coarse temporal and spatial resolutions. Snow survey network observations also allow for calibration and verification of the mathematical model.

The technique must rely solely on observations which are currently available in real-time in southern Québec(Canada), such as temperatures and precipitations measured at hourly (cooperative meteorological network of Québec) or daily (climatological network) time steps as well as surveys of the SWE and of the snow density measured manually at more or less two-week intervals. This means that we must rely on a rather simple snow model; more complex models such as SNTHERM (Jordan 1991) and CROCUS (Brun *et al.* 1992) or snow sublimation and snow drift algorithms (Pomeroy *et al.* 2002; Liston and Strurm 2004) must be discarded for data availability reasons.

In order to develop and validate this regional SWE analysis technique, a pilot study area and a snowpack model is selected. The calibration strategy for the model parameters plays a major role in this study. It has been divided into four parts: (1) calibration of the model parameters at each station of the snow survey network, (2) evaluation of the impact of the model time step and of the meteorological station network, (3) the spatial and temporal verification of the calibration, and (4) the combined use of streamflow observations and of a hydrological model to adapt the model parameters to various types of vegetation cover. An assimilation technique is also presented together with a numerical application.

Studied zones and used dataset

The objective of the project is to develop a SWE analysis technique for the southern Québec area, which extends from 64° to 80° west and from 45° to 50° north (Figure 1). This technique is developed after a detailed analysis of a pilot study area, presented in Figure 2, which extends from 70° to 72° west and from 45° to 47° north. Only the sub-region south of the St. Lawrence River and the territory within the Canadian borders are considered. Annual precipitations for this area are approximately 1 000 mm, of which roughly one-third consists of solid precipitations. The snow season starts around the beginning of December and generally ends in April. Ground elevations vary from a few meters above mean sea level near the St. Lawrence River to slightly above 1 000 m for the mountain peaks located in the extreme south of the study area.

Figure 2 presents the 24 observation sites of the snow survey network which are within the pilot study area. Measurements are taken at these stations four to seven times a year, around 31 January, 28 February, 15 March, 31 March and, when necessary, around 15 April,

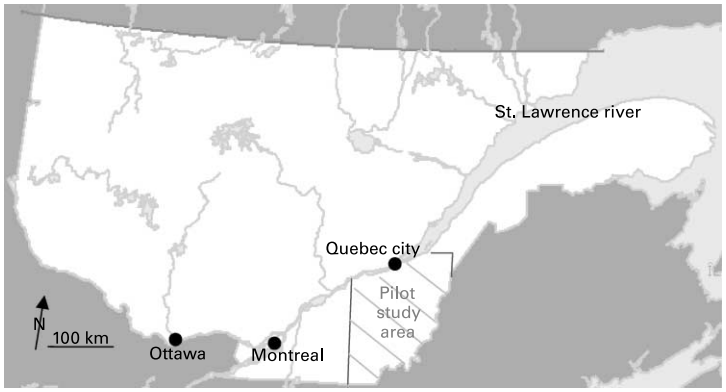

Figure 1 Targeted area for the operational application of the model (Southern Québec) and pilot study area

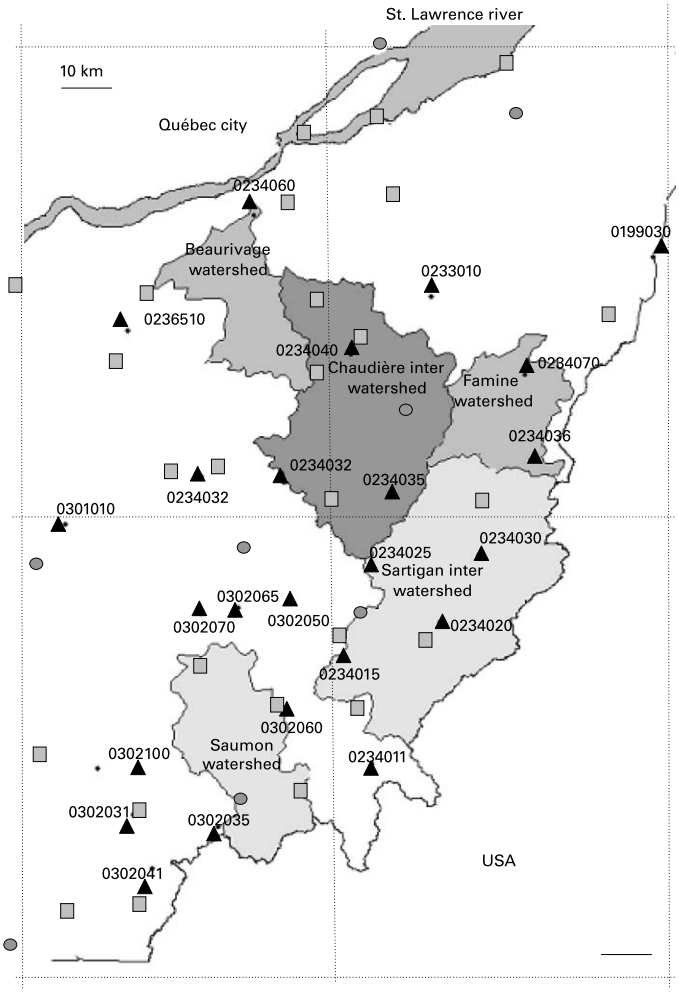

Figure 2 Observation sites of the snow survey network (triangle), automatic meteorological stations (circle) and climatological stations (square) in the pilot area

30 April and 15 May. The measurement sites are typically in open forest areas, where the evolution of the snow melt is comparable to that found in deciduous tree forests. Each observation consists in an average of ten measures taken manually with a snow tube on a deforested snow path that measures approximately 3 m in width and 300 m in length as proposed by WMO (World Meteorological Organization) 1994.

Figure 2 also presents the position of the two types of meteorological stations available in the pilot study area. The first set comprises the eight automatic stations with data available in real-time via telephone line or satellite. Air temperature and precipitation data, measured with a total precipitation gauge, are available at an hourly time step. The second set comprises the 27 stations belonging to the climatological network. For this network, data gathering and broadcasting are done twice a day by on-site observers. Daily variables are derived from those observations: minimum and maximum temperature, rainfall and snowfall, which is measured from a snow gauge. For climatic stations, snow is converted into its water equivalent, assuming an average density of 100 kg m^{-3} (Dingman 2002). The total precipitation gauges from the automatic stations are equipped with an "alter" windscreen but

there is no wind protection for the snow gauges of the climatological network. Hence, it is clear that solid precipitation estimations are under-estimated (Yang *et al.* 1999) in both networks. It is important to be aware that, for this study, we did not deal with this issue. Without wind speed measurements, it would have been difficult to accurately make the necessary adjustments (Fortin *et al.* 2006*b*) since corrections should vary from site to site. We consider that the impact of any error due to under-estimation is compensated by the assimilation of snow survey data and by the calibration of the snow model. In practice, this hypothesis can be verified by evaluating the bias of the analysis.

A second dataset that included 123 snow survey sites located within the southern Québec grid is used for the verification of the conclusions obtained for the pilot study area. These snow survey sites are located no more than 75 km from the nearest meteorological station.

Description of the snowmelt model

This section discussed the spatial resolution and the model choices. A detailed description of the model is also presented.

Choice of the spatial resolution

As indicated by Gray and Prowse (1992), the physiographic variables which describe the evolution of the snow cover are scale-dependent. At scales that are smaller than the regional scale (on the order of 10 km) variables, such as dominant wind, terrain roughness and detailed land-use, become important. However, this information is not available on an operational basis. Blöschl (1999) suggested that "optimum grid size may not exist and that the model element scale may in practice be dictated by data availability and the required resolution of the predictions". Weather and snow survey stations being almost always more than 10 km apart in Southern Québec, we hence decided upon a spatial resolution of 0.1° (roughly 10 km) for the snow analysis.

Choice of the model

Yang (2005) offers a good review of current snow models. Having only access to temperature and precipitation observations in real-time, complex models like SNTHERM (Jordan 1991) and CROCUS (Brun *et al.* 1992) models were quickly excluded, considering the input data required (short- and long-wave radiation, wind, relative humidity, etc.). Furthermore, it is important to note that the use of models like SNTHERM and CROCUS would have made the assimilation of snow survey data more complex since they divide the snowpack into many layers. These models are also more computationally costly.

Within the context of our study, only classical options based on a temperature index can be used with the meteorological data available operationally (Gray and Prowse 1992). There are many models based on a temperature index. The simplest solution is to base the melt estimates solely on the number of degree-days above a threshold and to use only SWE as a state variable. As shown by Xue (2003), the use of other state variables monitoring snow density and albedo seems helpful to obtain results that are closer to the actual evolution of the snow cover. This is the reason why some temperature index models take into account state variables of the snowpack, such as snow density, heat deficit and albedo. These models compromise algorithms which estimate the energy supply from solar radiation based on the air temperature. Due to the fact that these models take additional state variables into account, the possibility of assimilating snow water equivalent as well as snow depth exists.

The snow melt model of the hydrological model HYDROTEL (Fortin *et al.* 2001) which we chose to use for the present study falls into this last category of models based on a temperature index. It has one additional advantage, however: the HYDROTEL model has

been calibrated for various watersheds in southern Québec, and is used operationally for streamflow forecasting (Turcotte *et al.* 2002). This allows us to use the model to not only simulate the snow but also the streamflow which helps to improve the quality of the snow model parameters, by calibrating the snow model both on snow survey and streamflow data. This was a major operational advantage that leads us to choose HYDROTEL over other models of similar complexity.

By comparison with other snow models based on a temperature index and included in hydrological models, the HYDROTEL model is, in some respect, more sophisticated and in others less so. Among its weaknesses, the model does not take into consideration the interception of snow by the vegetation cover, as does DHSVM (Wigmosta *et al.* 2002) and ARC/EGMO (Becker *et al.* 2002). However, the processes simulated by HYDROTEL (air/snow and ground/snow interface melt, compaction, albedo evolution and liquid water retained by the snow cover) are much more complete than in other models. For example, WASMOD (Xu 2002) is limited to the direct use of a temperature index approach. In addition to the temperature index, HBV (Bergström 1992), DRAINMOD (Koivusalo *et al.* 2002) and CEQUEAU (Morin 2002) also include algorithms that consider the liquid water retention in the snow cover. ARC/EGMO and SSARR (Speers 1995) make use of state variables that can be linked to the heat deficit. It can also be said that HYDROTEL's approach for snow modelling is comparable, yet slightly different, to that of WATFLOOD (Kouwen *et al.* 1993). The latter was inspired by Anderson (1973) approaches, that are included in SAC-SMA (Burnash 1995), and Ambach (1988) methodology.

Model description

A description of the model is available in Fortin (2005). The model has five state variables: SWE, heat deficit, albedo, snow depth and liquid water retention within the snow cover. The algorithm assumes a single, homogeneous layer on the vertical.

The first component of the algorithm involves the partitioning of the total precipitation into liquid and solid precipitation. The partitioning depends on a threshold temperature at which rain becomes snow (0°C for the present study). When the maximum (resp. minimum) air temperature is below (resp. above) the temperature mentioned above, the total precipitation is assumed to be in solid (resp. liquid) form. When the maximum is above 0°C and the minimum is below 0°C, liquid and solid parts of the total precipitation are estimated by

$$R = P \cdot \left(\frac{T_{\max}}{T_{\min} - T_{\max}} \right) \tag{1}$$

$$S = P - R \tag{2}$$

where R is the liquid precipitation (m s^{-1}), S is the solid precipitation (m s^{-1}), P is the total precipitation (m s^{-1}), and $T_{\max}$ and $T_{\min}$ are, respectively, the maximum and minimum air temperatures on a time step (0°C). The following elements of the algorithm illustrate the evolution of two of the main variables, SWE and heat deficit. This is done using two equations, expressed as follows:

$$\frac{\Delta \mathrm{SWE}}{\Delta t} = \frac{\Delta \mathrm{WR}}{\Delta t} + R + S - M \tag{3}$$

and

$$\frac{\Delta U}{\Delta t} = u_s - u_r - u_c - u_{s-s}^{(P)} - u_{a-s}^{(P)} \tag{4}$$

where WR is the liquid water retained in the snow cover (m), M is melted water (m s^{-1}), U is the heat deficit (J m^{-2}), u_s is the increase in heat deficit due to solid precipitations (J m^{-2} s^{-1}),

u_r anf u_c are, respectively, decreases in heat deficit due to liquid precipitations and the loss of heat via convection (J m $^{-2}$ s^{-1}), $u_{s-s}^{(P)}$ and $u_{a-s}^{(P)}$ are, respectively, decreases in heat deficit due to the potential melt at the soil–snow interface and at the air–snow interface (J m^2 s^{-1}) and Δt is the time step (s^{-1}).

The calculation starts with the addition of the solid precipitation to the SWE and to the corresponding energy effect, calculated using the specific heat of the snow:

$$u_s = \rho_w C_s \frac{T_{\max} + T_{\min}}{2} s \tag{5}$$

where ρ_w is the density of the water (1 000 kg.m^{-3}) and C_s is the specific heat of the snow (2 093 J kg^{-1} °C^{-1}).

For time steps in which there are liquid precipitations, the water is added to the SWE. The heat deficit is also adjusted accordingly, as a function of the heat inflow to the snow cover from the precipitation and its associated temperature, which is assumed to be equal to the air temperature up to 0°C. In addition, the impact of the freezing of liquid precipitation on heat deficit is included in the equation:

$$u_r = \rho_w \left(C_f + C_w \frac{T_{\max} + T_{\min}}{2} \right) R \tag{6}$$

where C_f is the latent heat of fusion of water (334 000 J kg^1) and C_w is the specific heat of water (4 184 J kg^1 °C^1). In cases where the air temperature is below 0°C, the snow cover loses energy in the form of convection (u_c). We estimate this loss by using the classical solution of heat transfer in a semi-infinite medium with air temperature as limit condition (Dirichlet condition).

The heat provided at the surface of the soil is also considered and allows for a decrease in the heat deficit. In this model, the heat inflow to the snow, $u_{s-s}^{(P)}$, is defined by the following equation:

$$u_{s-s}^{(P)} = \frac{\mathrm{MR}_{s-s}}{86400} \rho_w C_f \tag{7}$$

where $\mathrm{MR}_{s\text{-}s}$ is the melt rate coefficient at the soil–snow interface (m d^{-1}) and 86 400 is the number of seconds in a day (s d^{-1}). As noted above, in order to use only the data which can be easily accessed, the external energy balance originating from solar radiation is evaluated with a method based on the temperature index. As such, solar radiation heat is estimated with the following equation, inspired directly from Riley *et al.* 1973:

$$u_{a-s}^{(p)} = \frac{\mathrm{MR}_{a-s}}{86400} \rho_w C_f \left(\frac{T_{\max} + T_{\min}}{2} - T_0 \right) (1 - a) \tag{8}$$

where $\mathrm{MR}_{a\text{-}s}$ is the melt rate coefficient at the air–snow interface (m d^{-1} °C^{-1}), T_0 is the temperature threshold at which melting occurs (°C) and a is the combined albedo of snow and vegetation. It is crucial to note that the results obtained from the above equation are potential melting rates that, along with the specific snow heat, are converted into heat intake. As such, it can be viewed as an estimation of the heat balance using a temperature index. If the heat balance of the snow cover is estimated to be positive using the above process, snow melt will occur in the model. This melting is estimated by dividing the heat surplus by the product of the melting heat, the water density and the time step:

$$M = \frac{-U}{\Delta t \rho_w C_f} \tag{9}$$

Water supplied by snowmelt can be retained in the cover, which acts as a porous media. As illustrated in the literature, capacity values for retention of the snow cover vary substantially (for reference, see Lefebre *et al.* 2003). This capacity was not calibrated and fixed at 10% of the snow depth, in the present model. If the retention capacity exceeds the melted volume, the melted water remains entirely retained within the cover. If the melted volume is greater than the retention capacity, the cover retains only the amount of water equivalent to the retention capacity. The difference appears as snow melt at the snow–soil interface.

In the model, the albedo is obtained as a weighted average of albedos of the solid precipitation layer, the snowpack layer and the vegetated soil layer. Weights are computed using an exponential expression approximating the exponential extinction of radiation penetration of snow (Tarboton and Luce 1996). For two consecutive layers, the weighting coefficient is given by

$$w = 1 - e^{-k/0.002} = 1 - w' \tag{10}$$

where k is the water equivalent of the solid precipitation (S) or the snowpack (SWE) and w and w' are the weigths to be used, respectively, for the upper and the lower layers. The previous equation is used to weight, on the one hand, the albedo of the solid precipitation with the albedo of the snowpack and, on the other hand, the albedo of the snowpack with the albedo of the soil. By combining this weighting approach and an exponential equation which takes into account the aging process (Fortin 2005), we define the albedo by the following equation:

$$a|_t = a_{\min} + \left(a_s w|_s + (1 - w|_s)\left(a|_{t-\Delta t} w|_{\mathrm{SWE}} + a_{\mathrm{soil}}(1 - w|_{\mathrm{SWE}})\right) - a_{\min}\right) e^{-0.2\Delta t/86400} \tag{11}$$

where a_s is the albedo of the solid precipitation ($a_s \cong 0.80$; Liston 1999), $a_{\min}$ is the lowest possible albedo for snowpack ($a_{\min} \cong 0.45$; Dingman 2002) and a_{soil} is the albedo of the vegetated soil ($a_{\mathrm{soil}} \cong 0.15$; Liston 1999). The model also simulates the snow depth evolution using the following equation:

$$\frac{\Delta \mathrm{SD}}{\Delta t} = S\frac{\rho_w}{\rho_s} - \mathrm{SDSC} - M\frac{\mathrm{SD}}{\mathrm{SWE}} \tag{12}$$

where SD is the snow depth (m), SC is the decrease factor of the snow depth on a time step (s^{-1}) and ρ_s is the density of the solid precipitation (kg m^{-3}) using

$$\rho_s = 151 + 10.63\left(\frac{T_{\max} + T_{\min}}{2}\right) + 0.2767\left(\frac{T_{\max} + T_{\min}}{2}\right)^2 \tag{13}$$

for $((T_{\max} + T_{\min})/2)$ between 0 and -17°C and $\rho_s = 50$ for $((T_{\max} + T_{\min})/2)$ under -17°C.

The decrease factor of the snow depth due to the compaction on a time step is proportional to the difference between the current density and the maximum possible density:

$$\mathrm{SC} = \frac{C_c}{86400}\left(1 - \frac{\mathrm{SWE} \cdot \rho_w}{\mathrm{SD}\rho}\right) \tag{14}$$

where C_c is the compaction coefficient (d^{-1}) and $\rho_{\max}$ is the maximum density of the snow (kg m^{-3}).

Model calibration

In practice, the parameters T_0, $MR_{s\text{-}s}$, $MR_{a\text{-}s}$, C_c and ρ_{max} of the model are subject to calibration. The current section presents the calibration process performed at the snow survey locations.

Precipitation and temperature interpolation

Before being able to produce simulations at the snow survey sites, precipitation and temperature must be interpolated at these locations. The interpolation is done with a simple averaging method: for each snow survey location, the three closest stations are identified and weighted proportionally to the inverse distance to the location of interest. A vertical temperature gradient of -0.5°C per 100 m of altitude (which approximates the average value of the saturated adiabatic gradient) is used to correct the temperatures prior to interpolation. No correction is made for altitude when interpolating precipitation.

Assimilation of snow survey observations for calibration

The assimilation of the snow survey observations during the course of the simulation is done by directly replacing the state variables, which represent the SWE and the snow depth, by observed values, when available. This method allows for corrections to be made to the model each time a new observation becomes available. The other state variables that are not measured (heat deficit, albedo, water retained in the snowpack) remain unchanged.

Model time step and meteorological station network for parameter calibration

It could be sufficient to simulate the evolution of the SWE at a daily time step, as this strategy would meet our operational requirements. However, a time step inferior to one day can be useful to capture the diurnal effects of the melting process. Brown *et al.* (2003), for example, study hourly simulations despite their final objective to establish daily outputs. We have decided to use three-hour time steps for this model instead of hourly time steps because of the availability of computer codes. The main disadvantage of our choice is the fact that there are few meteorological station networks that automatically record data at three-hour intervals, climatological stations being discarded.

Objective function

Data collected from the stations from the fall of 1999 until the summer of 2003 were used for calibration purposes. With respect to the data used specifically for the calibration, values indicative of 0 mm of SWE were added to both the 1 November and the 1 June data for each year to ensure coherent model behaviour before the period of snow accumulation and after the melting period. The added 0 mm values only served to calibrate and were set aside during the model performance analysis. The root mean square error (RMSE) between simulated and observed SWE was used as the objective function.

Calibration on snow density observations

The use of observed density at snow survey measurement sites can help choose reasonable values for some of the five calibration coefficients, thus reducing the number of degrees of freedom of the model. The coefficient was estimated using all snow density observations collected from 1908 to 2003 in Québec (42 822 readings). In order to discard outliers, a value of 466 kg/m^3, corresponding to the 99th percentile, was selected for ρ_{max}.

The compaction coefficient (C_c) and the melting rate at the soil–snow interface ($MR_{s\text{-}s}$) can also be adjusted based on snow density observations and on the sensitivity of simulated density to these two parameters. When the temperature is too cold to force melting at the snow–air interface and there is no precipitation, the increase in snow cover density in the

model depends on these two parameters. With the objective to reduce number of degrees of freedom, we choose to set the value of $MR_{s\text{-}s}$ at 0.59 mm d^{-1}, corresponding to the middle of the range proposed for this parameter in the literature (Gray and Prowse 1992). Calibration of model coefficients on snow density observations was thus limited to the compaction coefficient.

Because snow density changes when melt occurs, the parameters T_0 and $MR_{a\text{-}s}$ also influence the simulated density, and we opted for a preliminary sensitivity analysis of the compaction coefficient based on the RMSE between observed and simulated densities on the entire set of snow survey observations in the pilot region. After testing with different sets of possible values for T_0 and $MR_{a\text{-}s}$ (both to be subsequently calibrated), we realized that these two coefficients have a greater impact on density than does the compaction coefficient. This is illustrated by Figure 3, which presents the RMSE of the simulated snow density as a function of the compaction coefficient for various realistic pairs of the parameters T_0 and $MR_{a\text{-}s}$. The choice of the compaction coefficient is consequently of relatively low importance, but it is still important to use a reasonable value. Considering all tested pairs of T_0 and $MR_{a\text{-}s}$ as equally likely to produce accurate SWE simulations, we computed the average of the various traces (the white line in Figure 3), which we then minimized with respect to C_c. We found that making C_c equal to 0.01 leads to the lowest expected RMSE.

Calibration on snow water equivalent

The calibration of the two remaining coefficients (T_0 and $MR_{a\text{-}s}$) constitutes the central part of the calibration exercise. Two strategies are possible: either using the same, "global" parameter values for all sites, or using different, "local" values for each site. Because of the strong interaction which exists between T_0 and $MR_{a\text{-}s}$, and because of the limited number of observations available at each station, it is difficult to obtain meaningful coefficient values when calibrating both coefficients independently for each site. We therefore decided that the parameter T_0 would be kept constant for all sites, and that we would instead try either to use the same, global value for $MR_{a\text{-}s}$, or use a different, local value for each site. For the first option, the coefficients are estimated jointly by minimizing the total error over all snow survey measurement sites. The search for a minimum is achieved using a classical bi-dimensional search algorithm. The name given to the first optimization option is a "global–global" calibration strategy, because the same "global" coefficient value is used for

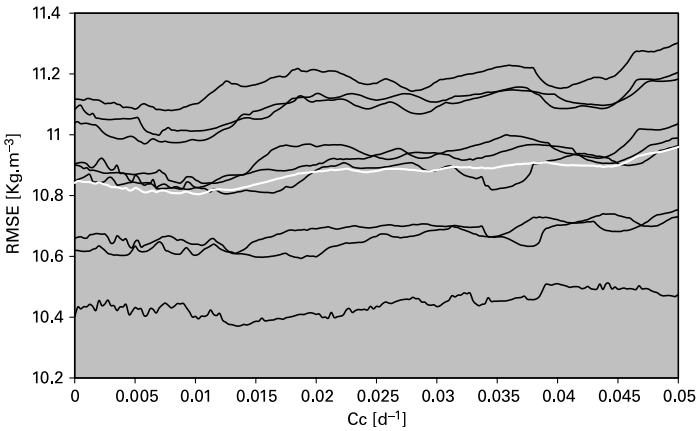

Figure 3 Simulated root mean square error (RMSE) for snowpack density as a function of compaction coefficients (C_c). Black lines stand for the results of different sets of coefficients ($MR_{a\text{-}s} = \{4,5,6\}$ mm d^{-1} °C^{-1}) and $T_0 = \{-1,0,1\}$°C), and the white line stands for the average of these results

all sites. For the second option, T_0 is calibrated globally by minimizing the total error over all snow survey measurement sites and $MR_{a\text{-}s}$ is calibrated according to an objective function evaluated independently at each site. This leads to a set of local $MR_{a\text{-}s}$ coefficients instead of a global one. In this case, an iterative approach is used for the optimization process, whereby the two calibration phases (for T_0 and $MR_{a\text{-}s}$) are alternated until the solution converges. This option is named the "global–local" calibration strategy.

There is an undeniable advantage in using a single coefficient set (resulting from the "global–global" calibration strategy), as it can be further used at every grid point without having to interpolate the parameters on the grid. On the other hand, it must be considered that focusing the calibration on each site for the "global–local" strategy could yield results that are significantly more accurate. The fact that local minimization is limited to only one parameter simplifies its regionalization, without having to worry about the coupling effect with other parameters.

Figure 4 illustrates that the objective function is a smooth function of T_0 and $MR_{a\text{-}s}$ for the "global–global" calibration strategy. Well known problems associated with functions having multiple local minima (Duan *et al.* 1992) or sensitivity to the convergence criterion (Isabel and Villeneuve 1986) for optimum search in hydrology can be avoided. As shown in Table 1, the coefficients leading to the lowest margin of error for the SWE are 1.6°C for T_0 and 6.4 $mm.d^{-1}\ °C^{-1}$ for $MR_{a\text{-}s}$. However, there is obviously a strong interaction between the coefficients.

The coefficient values obtained using the "global–local" calibration option are presented in Table 2. Values for the parameter $MR_{a\text{-}s}$ vary from 4.4 to 9.9 $mm\ °C^{-1}\ d^{-1}$, and a value of $T_0 = 1.7$°C is obtained for the threshold temperature coefficient.

Table 1 summarizes the errors originating from both calibration options (lines A and B) and also includes simulation results that will be discussed later (lines C to I). It should be noted also that the "global–local" minimization option reduces the RMSE and the mean absolute spread (MAS) by approximately 2 mm more than the "global–global" option. Mean relative spreads (not presented in Table 1) are 24.8% and 19.6%, respectively, for the "global–global" and "global–local" minimization options. Finally, the bias is very low (less

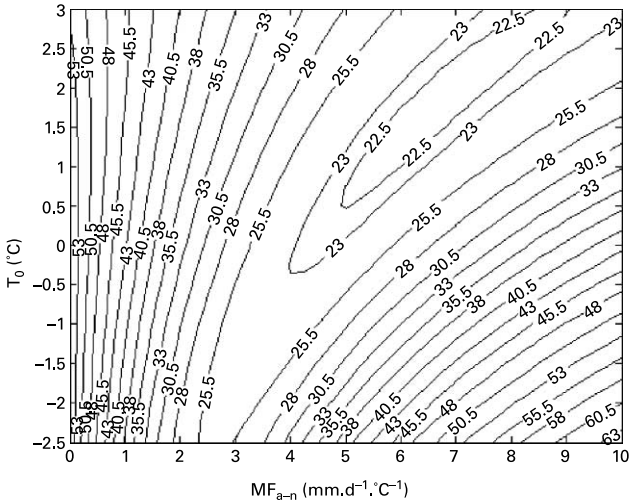

Figure 4 Simulated root mean square error (RMSE) for snowpack water equivalent (SWE) as a function of the melting rate coefficient at the air–snow interface ($MR_{a\text{-}s}$) and the temperature threshold coefficient (T_0) during the 1999–2003 time period for the "global–global" calibration strategy

Table 1 Errors on snow water equivalent in function of the strategy for coefficients determination, the set of coefficients, the meteorological stations, the time step and the time period

	Model	Strategy for coefficients determination	T_0 (°C)	Mran or MR (mm d^{-1} °C^{-1})	Studied area	Time period	Δt (h)	Meteorological network	RMSE (mm)	MAS (mm)	Bias (mm)
A	HYDROTEL	Calibration using "global–global" strategy. Resulting coefficients are named basic "global–global" coefficients	1.6	6.4	Pilot region	2000–2003	3	Automatic	25.7	18.5	−1.7
B	HYDROTEL	Calibration using "global–local" strategy Resulting coefficients are named basic "global–local" coefficients	1.7	Dependent on site (see Table 2, column A)	Pilot region	2000–2003	3	Automatic	23.5	16.7	−1.6
C	HYDROTEL	Calibration using "global–local" strategy	−0.4	Dependent on site (see Table 2, column B)	Pilot region	2000–2003	3	Automatic and climatologic	27.4	19.8	2.9
D	HYDROTEL	Calibration using "global–local" strategy	−1.1	Dependent on site (see Table 2, column C)	Pilot region	2000–2003	24	Automatic and climatologic	27.5	19.8	1.8
E	HYDROTEL	Interpolation of the MFan of the basic "global–local" coefficients set using the three nearest sites	1.7	Dependent on site (see Table 2, column D)	Pilot region	2000–2003	3	Automatic	25.5	18.4	−3.8
F	HYDROTEL	Direct use of the basic "global–global" coefficient set	1.6	6.4	Southern Québec	2002–2005	3	Automatic	35.4	25.3	−1.2
G	HYDROTEL	Calibration using "global–global" strategy	0.0	4.6	Pilot region	2004–2005	3	Automatic	28.7	22.5	−1.5
H	HYDROTEL	Direct use of the basic "global–global" coefficient set	1.6	6.4	Pilot region	2004–2005	3	Automatic	28.7	22.8	−1.5
I	Basic temperature index	Calibration of the MR	1.6	2.9	Pilot region	2000–2003	3	Automatic	26.8	19.7	−4.2

RMSE: root mean square error on SWE without zeros added in June and November; MAS: Mean absolute spread on SWE without zeros added in June and November; Bias: bias on SWE without zeros added in June and November; Δt: time step

Table 2 Melt rate coefficient at air–snow interface according to the snow survey observation sites and the various calibration options

		A **"Global–local" calibration** **Automatic** **3 h**	**B** **"Global–local" calibration** **Automatic and climatological** **3 h**	**C** **"Global–local" calibration** **Automatic and climatological** **24 h**	**D** **Interpolation** **Automatic** **3 h**
	Strategy				
	Meteorological stations	**1.7°C**	**−0.4°C**	**−1.1°C**	**1.7°C**
	Time step	**MR_{an}**	**MR_{an}**	**MR_n**	**MR_{an} (mm °C^{-1} d^{-1}) and**
	T_s	**(mm °C^{-1} d^{-1})**	**(mm °C^{-1} d^{-1})**	**(mm °C^{-1} d^{-1})**	**(relative error)**
Snow survey observation sites	199030	5.0	4.2	4.2	6.4 (−24%)
	233010	6.3	4.8	4.7	6.4 (−1%)
	234011	4.4	3.5	3.4	7.0 (−45%)
	234015	7.3	5.1	5.2	7.6 (−3%)
	234020	4.4	3.4	3.4	7.9 (−57%)
	234025	5.9	4.3	4.2	6.3 (−6%)
	234030	9.9	6.4	6.6	6.1 (47%)
	234032	8.8	6.1	6.0	8.4 (5%)
	234035	6.7	4.6	4.5	6.6 (2%)
	234036	7.9	5.8	6.1	7.1 (10%)
	234040	7.1	5.2	5.0	7.2 (−2%)
	234060	5.0	3.8	4.0	6.3 (−23%)
	234070	5.2	4.7	4.9	6.8 (−25%)
	236510	5.5	6.1	6.0	6.2 (−12%)
	240020	7.7	5.4	5.4	7.9 (−3%)
	301010	5.7	4.7	4.8	6.3 (−9%)
	302031	6.8	4.9	4.0	7.1 (−5%)
	302035	7.1	4.4	4.1	7.1 (0%)
	302041	8.2	4.9	4.4	6.7 (20%)
	302050	8.2	7.7	6.4	8.5 (−3%)
	302060	8.5	6.2	6.5	8.2 (3%)
	302065	9.4	6.8	7.0	7.0 (29%)
	302070	5.5	4.6	4.5	8.7 (−45%)
	302100	6.1	4.4	3.4	7.2 (−16%)

than 2 mm). This is an interesting feature for hydrological forecasting purposes, especially when snow analyses serve as an initial condition for ensemble streamflow predictions. It also indicates that the analysis does not suffer too much from the fact that the precipitation measurements are not corrected for wind-induced losses. Figures 5 and 6 allow the comparison between the resulting series obtained from both calibration options. Obviously, the gains derived from the "global–local" calibration option are detectable but minimal. Errors on SWE stay under 10, 20 and 50 mm, respectively 41%, 61% and 94% of the time when the "global–global" option is used and 45%, 65% and 96% when the "global–local" option is used.

Impact of calibration choices

One possible reason for obtaining, with the "global–local" calibration strategy, results that are not clearly better than with the "global–global" calibration strategy is that we have discarded a lot of input data by only using automatic weather stations. Recalling that climate observations are available at a 24 h time step, we have two options to assess the impact of using all of the available meteorological input data: either run the model at a 24 h time step, aggregating the data from the automatic stations, or keep running the model with a 3 h time step, by first disaggregating the observations from the climatological stations.

For this last option, it is necessary to pre-process the data from the climatological stations. The strategy used consists in dividing the daily total precipitations in eight and linearly interpolating the temperatures between the daily maximum value, assuming that it occurs at 3 o'clock PM, and the daily minimum value, assuming it occurs at 3 o'clock AM. Clearly, these estimations are not perfect. Nonetheless, in the context whereby daily results are final goals and the use of a 3 h time step is mainly a modeling strategy, the impact of the disaggregation is expected to be negligible for a daily snow water equivalent analysis.

Table 1 shows that for the "global–local" calibration strategy (line C), using both automatic and climatological stations deteriorates the quality of the results. Results are even worse when using a 24 h time step for the model (line D), which means that the disaggregation approach is better than the aggregation approach for using the climate stations. Consequently, it seems preferable to rely only on automatic stations at a 3 h time

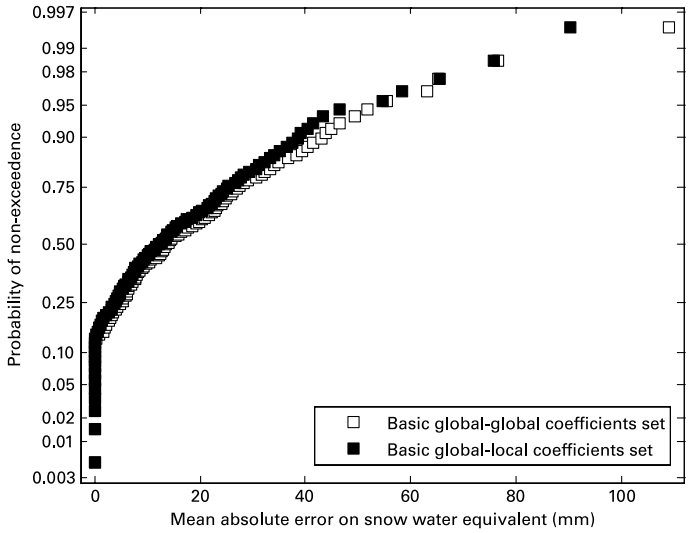

Figure 5 Probability of non-exceedence of a given mean absolute error on simulated snowpack water equivalent (SWE) for basic "global–global" and basic "global–local" coefficient sets

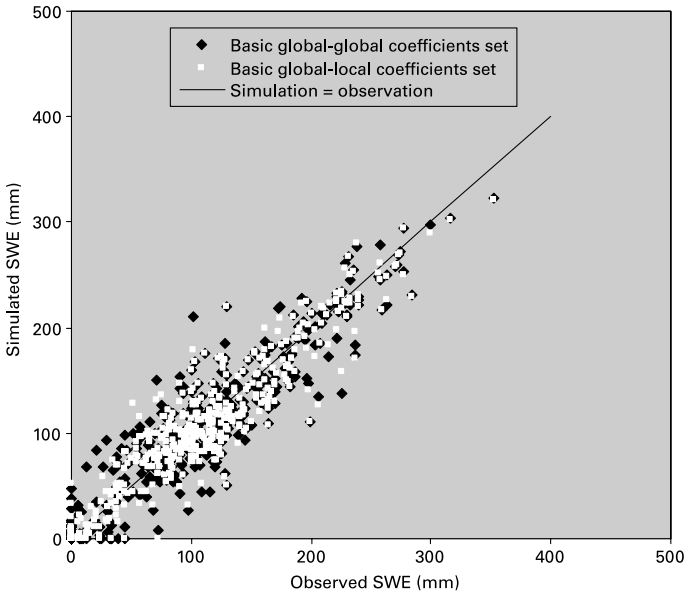

Figure 6 Scattered plot of simulated snowpack water equivalent (SWE) against observed SWE for basic "global–global" and basic "global–local" coefficient sets

step for operational purposes. It may seem surprising but the accuracy of solid precipitation measurement on the climatological network is lower, recalling that snow gauges have no wind protection and use a basic 100 kg m^{-3} density conversion. This conclusion should be applicable to southern Québec as a whole, since the pilot study area contains the highest ratio of climatological stations compared to automatic stations.

We already noted that the results obtained for the "global–global" and "global–local" calibration strategies are more or less equivalent (the "global–local" strategy being only slightly better), and we have shown that the results for the "global–local" strategy is not improved by including the climate stations in the analysis. The use of the "global–local" calibration strategy for every grid point, and not only snow survey sites, would further require the development of a regionalization technique to be applicable. We have tried a simple interpolation scheme for $MR_{a\text{-}s}$ and shown by cross-validation that the resulting simulations do not improve upon the "global–global" calibration strategy (Table 1, line E). We therefore recommend that the "global–global" method be used operationally, and that the same coefficient values be used on every grid point.

Spatial and temporal verification of the calibration, and impact of the model complexity

In order to verify if the use of the coefficient values estimated for the pilot region is applicable elsewhere in Québec, numerical tests were performed using all the available sites of the snow survey network within the limit of the grid for a four-year period. As shown in Table 1 (Line F), the use of these "global–global" parameter values for other basins leads to a RMSE of 35 mm while keeping the bias very low. By comparison, RMSE is roughly 20 mm on SWE for a sub-region in southern Québec using snow survey observations with kriging as the interpolation technique (Tapsoba *et al.* 2005). That RMSE value is obtained when the ratio between the number of observation sites and the domain area in Tapsoba *et al.* (2005) is equivalent to the one used in this study. It should be noted that the RMSE calculated by interpolation includes only spatial error. The RMSE calculated with our technique includes

both spatial and temporal errors since the error assessment is done at least 2 weeks after the last observation.

Table 1 also presents results for a temporal verification of the calibration (lines J and K). These results were taken over a two-year period (2004–2005), which was not used for parameter calibration. The error for the SWE, using coefficients calibrated in the 1999–2003 period (line K), is almost the same as the error associated with the parameters calibrated on the 2004–2005 period (line J).

Finally, the current model, which includes energy budget algorithms, is compared with a simpler temperature index model. The simpler model is defined by the following two equations:

$$\frac{\Delta \mathrm{SWE}}{\Delta t} = S - M \tag{15}$$

and

$$M = \frac{\mathrm{MR}}{86400}\left(\frac{T_{\max} + T_{\min}}{2} - T_0\right) \tag{16}$$

where MR is the melt rate coefficient of the basic temperature index model (m d^{-1} $^{\circ}\mathrm{C}^{-1}$).

As shown in Table 1 (compare line I with line A), the RMSE obtained by calibrating MR and using $T_0 = 1.6^{\circ}\mathrm{C}$ is slightly higher than the one obtained with the "global–global" strategy, and the bias is clearly higher. This illustrates the small but positive contribution of the added complexity in the model. Finally, one should note that the value of MR is similar to the melt factor proposed by various researchers in more or less equivalent geographical regions (see Gray and Prowse 1992). Comparison between $\mathrm{MR}_{a\text{-}s}$ and MR is difficult since other equations and coefficients influencing the snowmelt in the more complex model have to be compensated solely by the MR coefficient in the basic model.

Adaptation of the parameters for various soil covers

Recall that the snow survey measurement sites are systematically located in areas where the behaviour, in terms of snow melting and accumulation, is comparable to that in areas having deciduous trees. Especially for hydrological forecasting purposes, but also for other applications, it is useful for the model to represent snow accumulation and melt for all types of land cover, not only deciduous forest, through adapted model parameters. Since no water equivalent observation is available for other land covers, a direct estimation of the coefficients through calibration is not possible.

One possibility is to adapt model parameters by comparing observed with simulated streamflow using a hydrological model that takes into account land cover when simulating snowmelt. The operational hydrological model HYDROTEL discriminates between three classes of land cover: deciduous forest, coniferous forest and open areas, and simulates snow accumulation and melt independently for each of these three broad classes of land cover. We can therefore use HYDROTEL to determine if we can improve hydrological simulations by using different model coefficients for the snow model for each of the three classes of land cover. In order to do this, we have used the complete HYDROTEL model, instead of only the snow model, on a few watersheds in the pilot study area.

The methodology used to estimate the snow model parameters of the hydrological model relies on two key steps. First, the model is fully calibrated with streamflow data, independently for each of the drainage basins included in Table 1, using the SCE-UA algorithm (Duan *et al.* 1992) embedded within the algorithm proposed by Turcotte *et al.* (2002). This first calibration step allows us to establish the general performance of the model for all hydrological processes including the accumulation and melting of snow.

During that first step, the compaction coefficient C_c, the maximum density ρ_{max} and the melting rate at the soil–snow interface $MR_{s\text{-}s}$ are not calibrated but set at the values used previously. These values are used for the three classes of land cover since only the melting rate at the air–snow interface $MR_{a\text{-}s}$, and the temperature threshold at which melting occurs, T_0, can be adjusted to account for land cover within HYDROTEL. The melting rate at the air–snow interface and the temperature threshold for deciduous trees is also set at the values obtained from the "global–global" calibration strategy. This means that the only coefficients of the snow model which are calibrated are $MR_{a\text{-}s}$ and T_0 for coniferous forests and open areas.

As a second step, the calibration was then refined for the melting temperature used in coniferous forests and open areas, which we denote respectively by $T_0^{(CF)}$ and $T_0^{(OA)}$. In order to reduce further the parameter space, we assumed that $T_0^{(CF)}\text{-}T_0 = T_0\text{-}T_0^{(OA)} = \Delta t_0$, i.e. that the difference in the melting temperatures in coniferous vs deciduous forests was equal to the difference in the melting temperatures used in deciduous forests vs open areas. Then, Δt_0 was calibrated by minimizing the root mean square error during spring (1 March to 1 June).

As presented in Table 3, the estimated value for Δt_0 varies between 1.2°C to 2.8°C. One should also note that, with the exception of the value estimated for the Beaurivage watershed, the value estimated for Δt_0 varies only between 2.1°C and 2.8°C. This result gives us good confidence in the approach. The median value of 2.2°C is recommended for operational use.

A complete verification of the approach cannot be achieved since measurements of water equivalents at locations that are representatives of open areas and coniferous areas are not available. The only independent snow observations we could obtain for verification are measurements obtained for a research project at an agricultural site (Fortin *et al.* 2004). As shown in Figure 7, simulations and observations of water equivalent for the year 2004 are not very different. Furthermore, the model performance is increased by using a T_0 adjusted for open areas when compared to model performance using the non-adjusted value of T_0. It should be mentioned that observed values were obtained using the only point for snow tube measurements that was considered by the research team as representative of open areas in the region.

Assimilation of snow survey data

In the previous sections we have described in detail the complete computational process for simulating SWE on three grids corresponding to three different land uses. This process relies on a snow model that makes use solely of observed precipitation and temperature as input data. We also need an assimilation technique to update the state variables of the snow model based on observations from the snow survey network.

Slater and Clark (2006) and Clark *et al.* (2006) have been developed assimilation techniques based on the Kalman filter. Barrett (2003) proposed a simple Newtonian

Table 3 Adjustment coefficient for temperature threshold obtained by calibration on spring stream flows

Watershed	Area (km^2)	Localization (upper latitude; lower latitude; left longitude; right longitude)	Land uses (% of coniferous; % of deciduous; % of open areas)	Adjustment coefficient for temperature threshold (°C)
Famine	691	46.4; 46.1; −70.7; −70.2	41;43;16	2.8
Beaurivage	709	46.8; 46.3; −71.6; −71.0	19;44;37	1.2
Sartigan inter	2 295	46.2; 45.5; −71.0; −70.2	21;64;15	2.3
St.Lambert Inter	2 059	46.6; 45.9; −71.3; −70.6	20;42;38	2.2
Saumon	738	45.8; 45.2; −71.5; −71.0	12;52;36	2.1

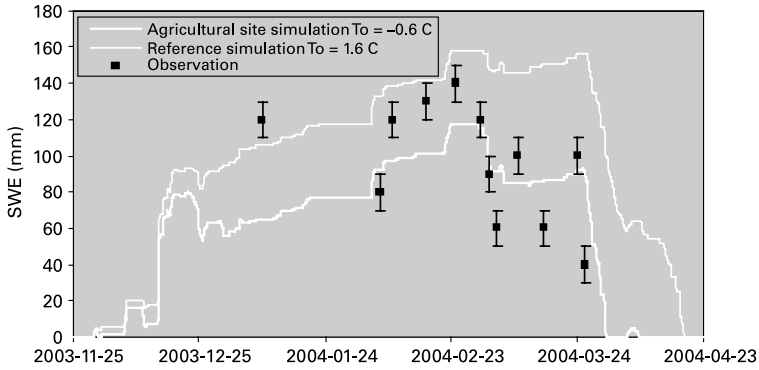

Figure 7 Comparison between observed and simulated snowpack water equivalent (SWE) for an agricultural site located at 46.3°N and 71.1°W using $MR_{a\text{-}s} = 6.4$ mm d^{-1} °C^{-1} and $T_O = -0.6$°C for the main simulation and $T_O = 1.6$°C for the reference simulation. The bars present the measurement errors

relaxation scheme which needs manual analysis to identify regions to update. These techniques are designed for the assimilation of remote sensing data and daily ground observations. The development of a technique that is especially designed for assimilation of snow survey data and that is completely automatic is still needed. Three key challenges must be considered for those propose: (1) spatial interpolation, (2) temporal synchronization of the error between observation and simulation and (3) transposition of the error from one land cover class to another.

Since locations of grid points do not generally correspond to the locations of snow survey observation sites, a spatial interpolation technique needs to be implemented. A simple weighted mean, with weights inversely proportional to the distance, was used. The interpolated values are errors computed at each snow survey observation site. The error is defined as the difference between simulated and observed SWE or snow density, depending on which state variable is updated (Barrett 2003). An error-based correction preserves the spatial pattern in the snowpack distribution induced by precipitation and temperature inputs, as well as by simulated snowmelt, while including information coming from the snow survey network.

The use of a weighting technique implies that more than one neighbouring snow survey observation site contributes to updating the SWE or snow density value at any given grid point. Since data are not always available at the exact same date for those neighbouring observation sites, a synchronization technique is needed. A first step is to define the neighbouring sites for each grid point by choosing the six closest snow survey observation sites. We then decided to set, for each grid point, the days in the winter season at which corrections should ideally be made. This decision was based on the dates at which the observers are expected in the region, assuming that updating should not necessarily be done at the same time all over the grid. To establish the exact day on which a correction is made at a grid point, we must then balance the requirement to use the most recently observed data as soon as possible, on the one hand, with the advantages of including the largest possible number of neighbouring observation sites by accepting to wait a few days for more data to become available. We decided to allow for a waiting period of a maximum of 5 d, following the date of the first measure at one of the neighbouring sites. This choice is based on the fact that technical staff normally tours a region within one business week. At the end of the waiting period, if one or more observations are still not available the correction is done using only the available sites. The weighted mean of the errors, synchronized at the date of the last available site, is used for correcting simulated values.

Most snow survey sites won't report an observation at the dates at which we finally decide to make a correction. To estimate the model error, a simple strategy is to compare two parallel simulation runs at each snow survey observation site. For the first run, SWE and snow density is updated each time an observation becomes available at the site. For the second simulation run, corrections are delayed by one observation, i.e. it is only when the next observation becomes available that the current observation will be used to update the SWE and snow density. This second run is used as a reference simulation to assess the model error at the snow survey sites: the difference between simulated values of the two parallel runs can indeed be interpreted as an indicator of the temporal evolution of the simulation error at one given time. This error, which we refer to as δ, is the increment that is interpolated on the grid and then used to correct the values simulated on the grid. Figure 8 illustrates the algorithm applied to SWE updating. The same approach is used for snow density.

This assimilation technique is only readily applicable to deciduous forested areas, as no observations are available operationally for coniferous forests and open areas. The simplest strategy for the other land cover classes is to apply the same correction to all land cover classes. During the snow accumulation period, this is coherent with the modelling approach as the parameters of the snow model which depend on land cover are not active. During the melting period, this strategy can be motivated as follows for SWE: when a linear relationship exists between simulated snow melt and air temperature in a snow model, then adjusting the SWE is equivalent to adjusting observed air temperature, a strategy commonly used by forecasters to adjust the internal state variables of a hydrological model during snowmelt (WMO (World Meteorological Organization) 1992). If the air temperature is assumed to be

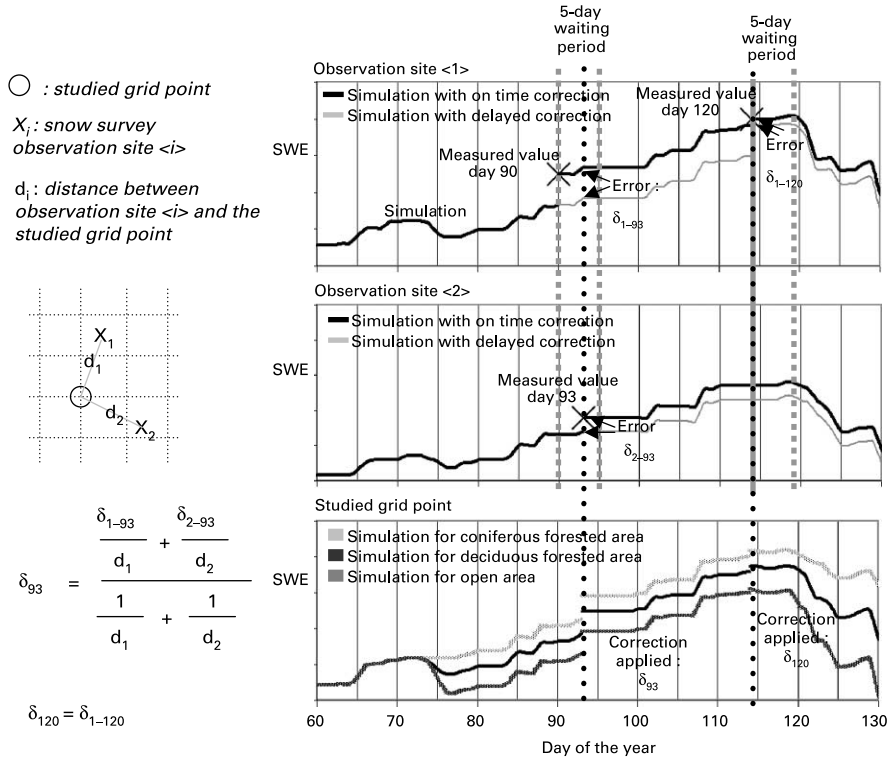

Figure 8 Schematic of the assimilation technique for a given grid point using, for simplification purposes, the two nearest snow survey sites as contributing neighbors for the correction

Table 4 Contribution of the snow analysis to the reduction of simulated streamflow errors for the 2005 spring flood simulation

	St-Lambert		Famine	
	Bias $m^3/s.d$	**RMSE m^3/s**	**Bias $m^3/s.d$**	**RMSE m^3/s**
	Simulation from 15 March to 1 June			
No assimilation	6.6	110.6	11.1	26.3
Assimilation on 15 March using the snow analysis for deciduous forested areas only	5.8	123.7	6.9	23.3
Assimilation on 15 March using snow analysis for three land use classes	2.0	111.9	7.0	21.9
	Simulation from 5 April to 1 June			
No assimilation	31.9	80.3	18.5	25.0
Assimilation on 5 April using the snow analysis for deciduous forested areas only	14.1	63.0	11.4	22.2
Assimilation on 5 April using snow analysis for three land use classes	7.8	49.8	10.5	22.6

independent of land use, then it follows that the same correction should be made for all land cover classes if the snow model is linear with respect to temperature.

For the snow model used in this study, the hypothesis of a linear relationship between air temperature and snowmelt is acceptable when air temperatures are clearly above 0°C. For the transition period when the melt is starting and air temperature oscillates about 0°C, the model

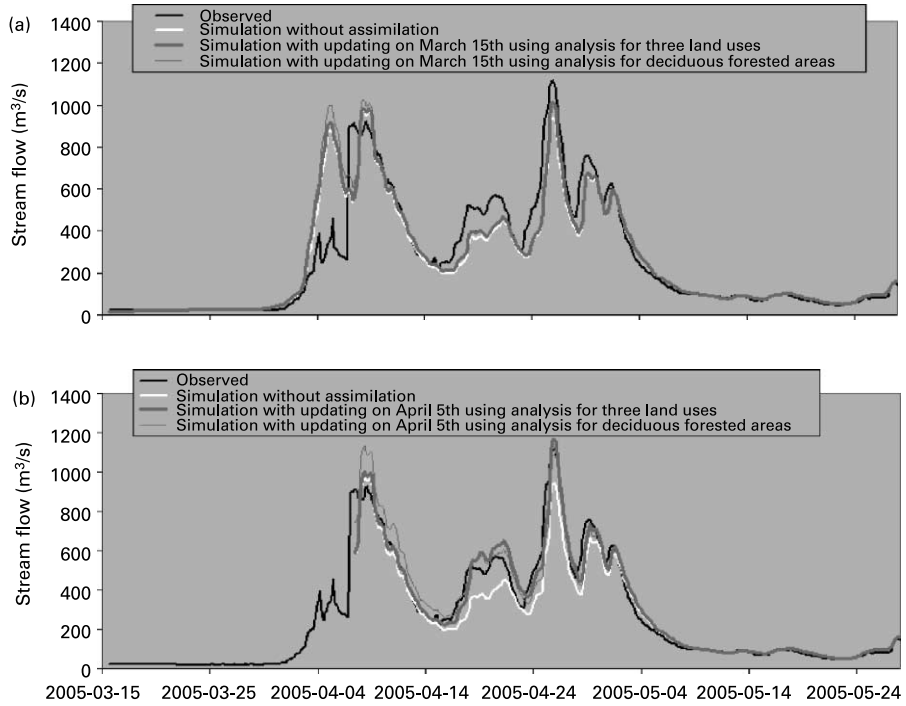

Figure 9 Comparison between observed and simulated stream flow at St-Lambert hydrometric station on the Chaudière River using assimilation of snow survey observations (a) on 15 March and (b) on 4 April

is nonlinear and therefore large corrections to the state variables of the model should be avoided if possible. It could be preferable in these cases to rerun the snow model by altering the temperature sequence to obtain the desired effect for the SWE in deciduous forests, and use these modified temperature sequence to force the snow model for the other land cover classes.

A direct validation of the assimilation technique is not easy. A numerical example showing the impact of the use of snow analysis on spring inflow forecasts can, however, serve to illustrate the usefulness of the snow analysis technique developed in this paper. Table 4 presents the bias of simulated inflows at the St-Lambert and Famine watersheds. As shown by Table 4, for the spring of 2005, the use of three different snow analyses for the three different land cover classes when updating modelled SWE and snow density leads generally to a reduction of errors on spring water yield, when compared to no assimilation of snow survey data or to an assimilation based on a unique value for all land cover classes. Hydrographs presented in Figure 9 for the St-Lambert watershed show that the simulation based on the more detailed snow analysis gives the best results. The presence of other hydrological sources of error in the simulated streamflow, such as errors on model structure, parameters identification and input data (Gupta *et al.* 2002), makes it difficult, however, to isolate the impact of the analysis on the quality of the hydrological simulation.

Conclusions

The objective of the study was to define an operational technique for the analysis of the spatio-temporal evolution of the water equivalent of the snowpack in southern Québec. The resulting technique combines the snow evolution model included in the hydrological model HYDROTEL with observed precipitation, temperature and snow survey observations. The model algorithm is based on a temperature index but still computes an energy budget using the air temperature to estimate the heat flux at the air–snow interface. Water equivalent, density and albedo of the snowpack, and liquid water retained in the snowpack, are the state variables of the model.

The identification of the five model parameters was one of the main challenges of the study. The melting rate at the soil–snow interface was obtained from a literature review. The parameter limiting the density of the snowpack and the coefficient which controls its compaction were calibrated using measured snow densities. More complex strategies were tested for the calibration of the melting rate at the air–snow interface and the threshold temperature for melt, which included attempts to have the melting rate vary in space. Still, results for the calibration period suggest that using the same parameter values for all grid points is preferable. Numerical results from independent spatial and temporal verification experiments confirmed that choice.

Numerical tests also demonstrated that forcing the model using observations from automatic stations at 3 h time steps is the best choice for operational needs: data from climate stations can be discarded. Finally, the adjustment of the threshold temperature for melt in open areas and coniferous forests was evaluated by comparing observed streamflows with the output from the complete HYDROTEL model. The final step was to develop an assimilation technique at the grid point scale using snow survey observations as the basic source of information. The approach proposed was illustrated on a case study, showing a positive contribution of the snow cover analysis to the accuracy of spring streamflow forecasts.

It should also be mentioned that an operational system is currently available based on the results of that study. The system has been operated in test mode since the spring of 2005. Daily operational results are available upon request to the first author. The analysis should be fully operational with results available on the internet during the spring of 2007.

In the future, we plan to compare this snow analysis technique with other techniques such as direct interpolation of snow survey observation data with kriging for example (Tapsoba *et al.* 2005). The distribution of errors associated with the proposed techniques will also be studied, with the objective to produce an ensemble of initial conditions for ensemble streamflow prediction. Recent experiments using the operational output of atmospheric models have provided us with some complementary information that could be included in the analysis. This approach, which was studied by Brown *et al.* (2003) and Fortin (2004), is particularly adapted for regions where there is a low density of meteorological stations. With the steady increase in the spatial resolution of short term numerical weather predictions, it is conceivable to use eventually as a first guess for the snow analysis the corresponding prognostic variable of a land surface scheme, such as CLASS (Verseghy 2000) or ISBA (Bélair *et al.* 2003) forced by atmospheric models or precipitation analysis derived from these models (Mahfouf *et al.* 2007). Remote sensing, particularly MODIS products, could also help verify the analysis in open areas.

Acknowledgements

The authors would like to thank Martin Beaudoin (IREQ), Stephanie Gottlieb (CEHQ), Charles Poirier (CEHQ), Pierre Lacombe (CEHQ), Stéphane Savary (INRS) Ali El Battay (CEHQ) and Diane Tremblay (INRS) for their help.

References

Ambach, W. (1988). Interpretation of the positive degree-day factor by heat balance characteristics – West Greenland. *Nordic Hydrol.*, **19**, 217–224.

Anderson, E.A. (1973). *National Weather Service River Forecast System – Snow Accumulation and Ablation Model*, NOAA Technical Memorandum NWS HYDRO-17, US Department of Commerce, Silver Spring, MD.

Barrett, A. (2003). *National Operational Hydrologic Remote Sensing Center Snow Data Assimilation System (SNODAS) Products at NSIDC*. NSIDC Special Report 11, National Snow and Ice Data Center, Boulder, CO, USA.

Becker, A., Klöcking, B., Lahmer, W. and Pfützner, B. (2002). The hydrological modelling system ARC/EGMO. In V.P. Singh and D.K. Frevert (Eds.), *Mathematical Models of Small Watershed Hydrology and Applications*, Water Resource Publications, Littleton, CO. pp. 321–384.

Bélair, S., Brown, R., Mailhot, J., Bilodeau, B. and Crevier, L.P. (2003). Operational implementation of the ISBA land surface scheme in the Canadian regional weather forecast model. Part II: Cold season results. *J. Hydrometeorol.*, **4**(2), 371–386.

Bergström, S. (1992). *The HBV Model – Its Structure and Applications*. SMHI Reports RH, No. 4, Norrköping.

Bernier, M., Fortin, J.P., Gauthier, Y., Gauthier, R., Roy, R. and Vincent, P. (1999). Determination of snow water equivalent using RADARSAT SAR data in eastern Canada. *Hydrol. Process.*, **13**(18), 3041–3051.

Blöschl, G. (1999). Scaling issues in snow hydrology. *Hydrol. Proc.*, **13**, 2149–2175.

Brasnett, B. (1999). A global analysis of snow depth for numerical weather prediction. *J. Appl. Meteorol.*, **38**, 726–740.

Brown, R.D., Brasnett, B. and Robinson, R. (2003). Gridded North American monthly snow depth and snow water equivalent for GCM evaluation. *Atmos.-Ocean*, **41**(1), 1–14.

Brown, R.D., Walker, A. and Goodison, B. (2000). Seasonal snow cover monitoring in Canada: an assessment of Canadian contributions for global climate monitoring. In: *57th Eastern Snow Conference, Syracuse, NY*.

Brun, E., David, P., Sudul, M. and Brunot, G. (1992). A numerical model to simulate snow cover stratigraphy for operational avalanche forecasting. *J. Glaciol.*, **38**, 13–22.

Burnash, R.J.C. (1995). The NWS river forcast system – catchment model. In V.P. Singh (Ed.), *Mathematical Models of Watershed Hydrology*, Water Resource Publications, Littleton, CO. pp. 311–366.

Carroll, T.R., Cline, D.W. and Li, L. (2000). Applications of remotely sensed data at the National Operational Hydrologic Remote Sensing Center. Presented at *IAHS Remote Sensing and Hydrology 2000, Santa Fe, NM, April 2–7*.

Clark, M.P., Slater, A.G., Barrett, A.P., Hay, L.E., McCabe, G.J., Rajagopalan, B. and Leavesley, G.H. (2006). Assimilation of snow covered area information into hydrologic and land-surface models. *Adv. Water Res.*, **28**(8), 1209–1221.

De Sève, D., Bernier, M., Fortin, J.P. and Walker, A. (2001). Estimation de l'équivalent en eau de la neige (EEN) à l'aide de données SSM/I pour un milieu de Taïga. *Télédétection*, **2**(1), 13–28.

Derksen, C., Walker, A. and Goodison, B. (2003). A comparison of 18 seasons of in situ and passive-derived snow water equivalent estimates in Western Canada. *Remote Sensing Environ.*, **88**, 271–282.

Dingman, S.L. (2002). *Physical Hydrology* (2nd ed.), Prentice-Hall, Englewood Cliffs, NJ.

Duan, Q., Sorooshian, S. and Gupta, V. (1992). Effective and efficient global optimization for conceptual rainfall-runoff models. *Water Res. Res.*, **28**(4), 1015–1031.

Fortin, V. (2004). *Simulation et prévision de la crue 2002 de la Gatineau avec différentes sources d'information météorologique*. Report, Institut de recherche d'Hydro-Québec.

Fortin, J.P. (2005). *Manuel de l'usager d'Hydrotel*, Rapport de recherche. INRS-ETE, Québec.

Fortin, J.P., Turcotte, R., Massicotte, S., Moussa, R., Fitzback, J. and Villeneuve, J.P. (2001). A distributed watershed model compatible with remote sensing and GIS data. Part I: description of the model. *J. Hydrol. Engng., ASCE*, **6**(2), 91–99.

Fortin, J.P., Turcotte, R., Savary, S. and Bernier, M. (2004). Forecasting streamflow from snow melt using the HYDROTEL model together with actual and simulated data from SNOWPOWER probes. In: *European Union of Geoscience, Nice, 25–30 April*.

Fortin, V., Therrien, C. and Anctil, F. (2006a). Correcting wind-induced bias in solid precipitation measurements using limited and uncertain data. *Hydrol. Process*. Submitted for publication.

Fortin, V., Turcotte, R. and Pellerin, P. (2006b). Improving medium-range ensemble streamflow forecasts by taking into account the uncertainty on the state of the snowpack. *2nd International Symposium on Quantitative Precipitation Forecasting and Hydrology, 4–8 June*. Poster.

Goïta, K., Walker, A.E. and Goodison, B.E. (2003). Algorithm development and use for the estimation of snow water equivalent in the boreal forest using passive microwave data. *Int. J. Remote Sensing*, **24**(3), 1097–1102.

Gray, D.M. and Prowse, T.D. (1992). Hydrologic forecasting. In D.R. Maidment (Ed.), *Handbook of Hydrology*, McGraw-Hill, New York. pp. 7.1–7.58.

Gupta, H.V., Sorooshian, S., Hogue, T.S. and Boyle, D.P. (2002). Advances in automatic calibration of watershed models. In: Duan, Q., Gupta, H.V., Sorooshian, S., Rousseau, A.N. and Turcotte, R. (Eds.). *Calibration of Watershed Models*. AGU Water Resources Monograph Series. DOI:10.1029/006WS02.

Isabel, D. and Villeneuve, J.P. (1986). Importance of the convergence criterion in the automatic calibration of hydrological models. *Water Res. Res.*, **22**(10), 1367–1370.

Jordan, R. (1991). *A One-dimensional Temperature Model for Snow Cover*. US Army Corps of Engineers, Cold Regions Research and Engineering Laboratory, New Hampshire, USA. Special Report 91-16.

Koivusalo, H., Kokkonen, T. and Karvonen, T. (2002). Modeling runoff from hydrologically similar areas. In V.P. Singh and D.K. Frevert (Eds.), *Mathematical Models of Large Watershed Hydrology and Applications*, Water Resource Publications, Littleton, CO, Chapter 18.

Kouwen, N., Soulis, E.D., Pietroniro, A., Donald, J. and Harrington, R.A. (1993). Grouping response units for distributed hydrologic modelling. *J. Water Res. Mngmnt. Plann., ASCE*, **119**(3), 289–305.

Lefebre, F., Gallée, H., Van Ypersele, J.P. and Greuell, W. (2003). Modeling of snow and ice melt at ETH Camp (west Greenland): a study of surface albedo. *J. Geophys. Res.*, **108**(D8), 4231.

Liston, G.E. (1999). Interrelationships among snow distribution, snowmelt, and snow cover depletion: implications for atmospheric, hydrologic, and ecologic modeling. *J. Appl. Meteorol.*, **38**(10), 1474–1487.

Liston, G.E. and Strurm, M. (2004). The role of winter sublimation in the Arctic moisture budget. *Nordic Hydrol.*, **35**, 325–334.

Mahfouf, J.F., Brasnett, B. and Gagnon, S. (2007). A Canadian precipitation analysis (CAPA) project. Description and preliminary results. *Atmos.-Ocean*, **45**(1), 1–17.

Morin, G. (2002). Cequeau hydrological model. In V.P. Singh and D.K. Frevert (Eds.), *Mathematical Models of Large Watershed Hydrology and Applications*, Water Resource Publications, Littleton, CO, Chapter 13.

Pietroniro, A., Fortin, V., Kouwen, N., Neal, C., Turcotte, R., Davidson, B., Verseghy, D., Soulis, R., Caldwell, R., Evora, N. and Pellerin, P. (2006). Using the MESH modelling system for hydrological ensemble forecasting of the Laurentian Great Lakes at the regional scale. *Hydrol. Earth Syst. Sci.*, **3**(4), 2473–2521.

Pomeroy, J.W., Gray, D.M., Hedstrom, N.R. and Janowicz, J.R. (2002). Physically based estimation of seasonal snow accumulation in the boreal forest. *Proc. Eastern Snow Conference*, **58**, 93–108.

Riley, J.P., Israelsen, E.K. and Eggleston, K.O. (1973). Some approaches to snowmelt prediction. *The Role of Snow and Ice in Hydrology*, IAHS pub 107, IAHS, Wallingford. pp. 956–971.

Romanov, P. (2003). Mapping and monitoring of the snow cover fraction over North America. *J. Geophys. Res.*, **108**(d16), 8619.

Roy, V., Goïta, K., Royer, A., Walker, A.E. and Goodison, B.E. (2004). Snow water equivalent retrieval in a Canadian boreal environment from microwave measurements using the HUT snow emission model. *IEEE Transactions on Geoscience and Remote Sensing*, **42**(9), 1850–1859.

Seidou, O., Fortin, V., St-Hilaire, A., Favre, A.C., El Adlouni, S. and Bobée, B. (2006). Estimating the snow water equivalent on the Gatineau catchment using hierarchical Bayesian modelling. *Hydrol. Proc.*, **20**(4), 839–855.

Simic, A., Fernandes, R., Brown, R., Romanov, P. and Park, W. (2004). Validation of VEGETATION, MODIS and GOES + SSM/I snow cover products over Canada based on surface snow depth observations. *Hydrol. Process.*, **18**(6), 1089–1105.

Slater, A.G. and Clark, M.P. (2006). Snow data assimilation via an ensemble Kalman filter. *J. Hydrometeorol.*, **7**, 478–493.

Speers, D.D. (1995). SSARR model. In V.P. Singh (Ed.), *Mathematical Models of Watershed Hydrology*, Water Resource Publications, Littleton, CO. pp. 367–394.

Tapsoba, D., Fortin, V., Anctil, F. and Haché, M. (2005). Apport de la technique du krigeage avec dérive externe pour une cartographie raisonnée de l'équivalent en eau de la neige: application aux bassins de la rivière Gatineau. *Can. J. Civil Engng.*, **32**(1), 289–297.

Tarboton, D.G. and Luce, C.H. (1996). *Utah Energy Balance Snow Accumulation and Melt Model (UEB). Computer Model Technical Description and User's Guide*. Utah Water Research Laboratory and USDA Forest Service Intermountain Research Station, available at: http://www.engineering.usu.edu/cee/faculty/dtarb/snow/snowreptext.pdf.

Turcotte, R., Rousseau, A.N. Fortin, J.P. and Villeneuve, J.P. (2002). A process-oriented, multiple-objective calibration strategy accounting for model structure. In: Duan, Q., Gupta, H., Sorooshian, S., Rousseau, A.N. and Turcotte, R. (Eds.). *Calibration of Watershed Models*. AGU Water Resources Monograph Series. American Geophysical Union, Washington, DC, DOI:10.1029/006WS11.

Verseghy, D.L. (2000). The Canadian Land Surface Scheme (CLASS): its history and future. *Atmos.-Ocean*, **38**(1), 1–13.

Wigmosta, M.S., Nijssen, B. and Storck, P. (2002). The distributed hydrology soil vegetation model. In V.P. Singh and D.K. Frevert (Eds.), *Mathematical Models of Small Watershed Hydrology and Applications*, Water Resource Publications, Littleton, CO, Chapter 2.

WMO (World Meteorological Organization) (1992). *Simulated Real-time Intercomparison of Hydrological Models*, WMO, Geneva.

WMO (World Meteorological Organization) (1994). *Data Acquisition and Processing, Analysis, Forecasting and Other Applications. Guide to Hydrological Practices* (5th ed.), WMO, Geneva.

Woo, M.K. and Young, K.L. (2004). Modeling arctic snow distribution and melt at the 1 km grid scale. *Nordic Hydrol.*, **35**, 295–307.

Xu, C.-Y. (2002). WASMOD – the water and snow balance modelling system. In V.P. Singh and D.K. Frevert (Eds.), *Mathematical Models of Small Watershed Hydrology and Applications*, Water Resource Publications, Littleton, CO, Chapter 17.

Xue, Y. (2003). Impact of parameterizations in snow physics and interface processes on the simulation of snow cover and runoff at several cold region sites. *J. Geophys. Res.*, **108**(d22), 8859.

Yang, D., Ishida, S., Goodison, B. and Gunther, T. (1999). Bias correction of precipitation data for Greenland. *J. Geophys. Res.-Atmos.*, **104**(D6), 6171–6181.

Yang, Z.L. (2005). Description of recent snow models. In: Martin, E. and Armstrong, R. (Eds.). *Snow and Climate*. International Committee on Snow and Ice, Oxford University Press, available at: http://www.geo.utexas.edu/climate/Research/SNOWMIP/snowmip.htm.